Dabrowiak, J. C. (1983) *Life Sci. 32*, 2915–2931.
Davanloo, P., Rosenberg, A. H., Dunn, J. J., & Studier, F. W. (1984) *Proc. Natl. Acad. Sci. U.S.A. 81*, 2035–2039.
Dervan, P. B. (1986) *Science 232*, 464–471.
Dunn, J. J., & Studier, F. W. (1983) *J. Mol. Biol. 166*, 477–535.
Eliades, A., Phillips, D. R., Reiss, J. A., & Skorobogaty, A. (1988) *J. Chem. Soc., Chem. Commun.*, 1049–1051.
Fox, K. R., & Waring, M. J. (1984) *Nucleic Acids Res. 12*, 9271–9285.
Fox, K. R., & Howarth, N. R. (1985) *Nucleic Acids Res. 13*, 8695–8714.
Fox, K. R., & Waring, M. J. (1986) *Biochemistry 25*, 4349–4356.
Fox, K. R., Brassett, C., & Waring, M. J. (1985) *Biochim. Biophys. Acta 840*, 383–392.
Gunderson, S. I., Chapman, K. A., & Burgess, R. R. (1987) *Biochemistry 26*, 1539–1546.
Hanahan, D. (1983) *J. Mol. Biol. 166*, 557–580.
Ikeda, R. A., & Richardson, C. C. (1986) *Proc. Natl. Acad. Sci. U.S.A. 83*, 3614–3618.
Low, M. L., Drew, H. R., & Waring, M. J. (1984) *Nucleic Acids Res. 12*, 4865–4879.
Maniatis, T., Fritsch, E. F., & Sambrook, J. (1982) *Molecular Cloning—A Laboratory Manual*, Cold Spring Harbor Laboratory, Cold Spring Harbor, NY.
Melton, D. A., Kreig, P. A., Rebagliati, M. R., Maniatis, T., Zinn, K., & Green, M. R. (1984) *Nucleic Acids Res. 12*, 7035–7056.
Neidle, S., & Abraham, Z. (1984) *CRC Crit. Rev. Biochem. 17*, 73–121.
Pardi, A., Morden, K. M., Patel, D. J., & Tinoco, I. (1983) *Biochemistry 22*, 1107–1113.
Phillips, D. R., & Crothers, D. M. (1986) *Biochemistry 25*, 7355–7362.
Shi, Y.-B., Gamper, H., & Hearst, J. E. (1987) *Nucleic Acids Res. 15*, 6843–6845.
Shi, Y.-B., Gamper, H., & Hearst, J. E. (1988) *J. Biol. Chem. 263*, 527–534.
Skorobogaty, A., Brownlee, R. T. C., Chandler, C. J., Kyratzis, I., Phillips, D. R., Reiss, J. A., & Trist, H. (1988a) *Anti-Cancer Drug Des. 3*, 41–56.
Skorobogaty, A., White, R. J., Phillips, D. R., & Reiss, J. A. (1988b) *FEBS Lett. 227*, 103–106.
Skorobogaty, A., White, R. J., Phillips, D. R., & Reiss, J. A. (1988c) *Drug Design Delivery 3*, 125–152.
Smeekens, S. P., & Romano, L. J. (1986) *Nucleic Acids Res. 14*, 2811–2828.
Straney, D. C., & Crothers, D. M. (1985) *Cell 43*, 449–459.
Studier, R. W., & Moffatt, B. A. (1986) *J. Mol. Biol. 189*, 113–130.
Tullius, T. D. (1987) *Trends Biochem. Sci. 12*, 297–300.
Van Dyke, M. W., & Dervan, P. B. (1983) *Biochemistry 22*, 2373–2377.
Van Dyke, M. M., & Dervan, P. B. (1984) *Science 225*, 1122–1127.
von Hippel, P. H., Bear, D. G., Morgan, W. D., & McSwiggen, J. A. (1984) *Annu. Rev. Biochem. 53*, 389–446.
White, R. J., & Phillips, D. R. (1988) *Biochemistry 27*, 9122–9132.

Laser Temperature-Jump, Spectroscopic, and Thermodynamic Study of Salt Effects on Duplex Formation by dGCATGC†

Alison P. Williams,‡ Carl E. Longfellow,‡ Susan M. Freier,‡ Ryszard Kierzek,§ and Douglas H. Turner*,‡
Department of Chemistry, University of Rochester, Rochester, New York 14627, and Institute of Bioorganic Chemistry, Polish Academy of Sciences, 60-704 Poznan, Noskowskiego 12/14, Poland

Received October 13, 1988; Revised Manuscript Received January 25, 1989

ABSTRACT: Salt effects on duplex formation by dGCATGC have been studied with spectroscopic, thermodynamic, and kinetic methods. Circular dichroism spectra indicate different salt conditions have little effect on the structures of the duplex and single strand. NMR chemical shifts indicate the structure of the duplex in 1 M NaCl is similar to that of the B-form determined previously in 0.5 M KCl [Nilges, M., Clore, G. M., Gronenborn, A. M., Brunger, A. T., Karplus, M., & Nilsson, L. (1987) *Biochemistry 26*, 3718–3733]. Optical melting experiments indicate the effect of Na^+ concentration on melting temperature is similar to that expected for a polynucleotide with the same GC content. Laser temperature-jump experiments indicate the effect of Na^+ concentration on the rate of duplex formation is much less than is observed for polynucleotides. The observations are consistent with expectations based on a counterion condensation model. This is surprising for a duplex with only 10 phosphates.

The salt dependence of duplex formation by short nucleic acids is important for the prediction of nucleic acid structure and dynamics under different buffer conditions. An understanding of salt effects is also important for the interpretation and prediction of the influence of salt on processes that may involve formation of short duplex regions. Such processes include RNA processing and control of gene expression by "antisense" nucleic acids. For example, reactions of both RNase P (Altman et al., 1986) and the self-splicing RNA from *Tetrahymena thermophila* (Cech, 1987) have been shown to depend on salt in unusual ways (Reich et al., 1988; Sugimoto et al., 1988). Effects of site-directed mutagenesis that disrupts base pairing can also be dependent on salt. For example, Burke et al. (1986) found that disrupting conserved pairs in

† This work was supported by National Institutes of Health Grant GM22939 (D.H.T.). A.P.W. was partially supported by an NSF Predoctoral Fellowship and the National Organization for the Professional Advancement of Black Chemists and Chemical Engineers.
‡ University of Rochester.
§ Polish Academy of Sciences.

0006-2960/89/0428-4283$01.50/0

the self-splicing RNA from *T. thermophila* eliminates activity at 2 mM Mg^{2+} but not at 10 mM Mg^{2+} in the presence of 0.1 M $(NH_4)_2SO_4$.

Considerable experimental and theoretical work exists on the salt dependence of duplex formation by polymers (Record et al., 1978; Manning, 1978). In contrast, little is known about the effects of salt on the behavior of oligonucleotides (Pörschke et al., 1973; Elson et al., 1970; Freier et al., 1984; Record & Lohman, 1978; Erie et al., 1987). For polymers, the observed effects are explained by counterion condensation and Poisson–Boltzmann theories that are thought to apply for helixes of lengths ≥15 nucleotides (Manning, 1976, 1978; Record et al., 1978). It is not clear, however, how well these theories describe oligomer behavior. This paper reports the thermodynamic and kinetic properties of dGCATGC as a function of Na^+ and Mg^{2+} concentrations. The results are compared with the salt dependence expected for a polymer of comparable base composition.

Materials and Methods

Oligonucleotide. dGCATGC was synthesized on solid support with a phosphoramidite method (Beaucage & Caruthers, 1981; Matteuchi & Caruthers, 1981; Barone et al., 1984). The molecule was purified by high-performance liquid chromatography (HPLC)[1] on a PRP-1 column (Ikuta et al., 1984) and deblocked. Purity was rechecked by HPLC on a C8 column in 0.05 M Na_2HPO_4 and 0.05 M NaH_2PO_4, pH 6.8, using a gradient from 0 to 25% methanol.

Circular Dichroism. CD spectra were measured at 0 and 70 °C with a Jasco J-40 spectropolarimeter. The strand concentration was 1.32×10^{-4} M, and the cell path length was 1 mm.

NMR. NMR spectra were measured on a Brucker WH 400-MHz instrument. The sample was 6.63×10^{-4} M dGCATGC in D_2O with 1 M NaCl, 0.01 M sodium cacodylate, and 0.001 M EDTA, pH 7. TSP was used as an internal standard. Temperature was determined from plots of the change in chemical shift of TSP relative to HDO as a function of temperature.

Thermodynamics. Solutions were buffered at pH 7 with 10 mM sodium cacodylate and also contained 0.1 mM Na_2-EDTA. Concentrations given for Mg^{2+} refer to Mg^{2+} in excess of EDTA. Prior to dilution of oligonucleotide for experiments, buffers were degassed by heating to 90 °C for 10 min. Absorbance versus temperature melting curves were measured at 260 and 280 nm on a Gilford 250 spectrophotometer at a heating rate of 1 °C/min as described previously (Hickey & Turner, 1985). Thermodynamic parameters for helix formation were determined by two methods. First, $\Delta H°$ and $\Delta S°$ were derived by fitting individual curves to a two-state model with linear sloping base lines and averaging the results for a range of oligomer concentrations (Petersheim & Turner, 1983). The melting temperature, T_M, where half of the strands are in duplex was also determined this way for each curve. For a self-complementary sequence, $T_M^{-1} = (2.3R/\Delta H°) \log C_T + \Delta S°/\Delta H°$, where C_T is the total concentration of strands. Thus, second, T_M^{-1} was plotted vs log C_T, and the values for $\Delta H°$ and $\Delta S°$ were derived from the slope and intercept of this line (Borer et al., 1974).

Strand concentrations were determined at 260 nm from the sample absorbance at high temperatures. The extinction coefficient at 260 nm was calculated to be 55 200 M^{-1} cm^{-1} for single strands by using the nearest-neighbor approximation method described by Richards (1975) and Borer (1975). The extinction coefficients are independent of salt concentration.

[1] Abbreviations: CD, circular dichroism; EDTA, ethylenediaminetetraacetic acid; HPLC, high-performance liquid chromatography; NMR, nuclear magnetic resonance; TSP, sodium 3-(trimethylsilyl)-tetradeuteriopropionate.

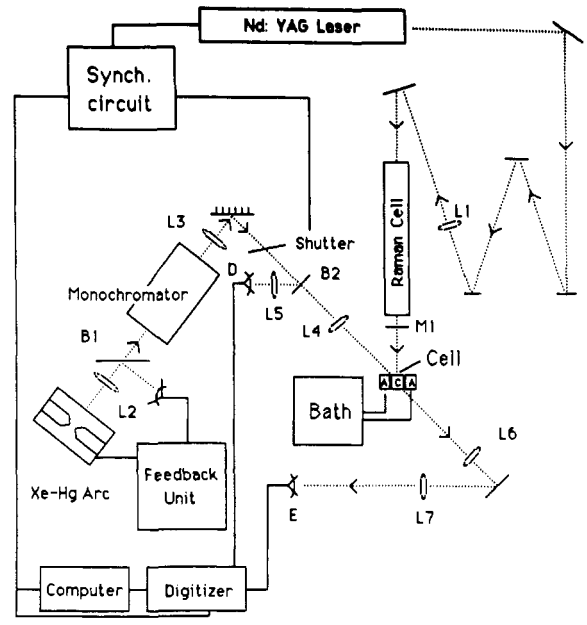

FIGURE 1: Block diagram of Raman laser temperature-jump apparatus: Synch. circuit, synchronizes all components and the data collection; L, lenses; B, beam splitters; M1, dielectric mirror reflecting 100% at 1.06 μm; A, thermostated cell holder; C, sample cell; D, reference photomultiplier; E sample photomultiplier. Not shown are Schott UG5 filters in front of each photomultiplier. Each photomultiplier is also followed by an amplifier with adjustable gain.

Temperature Jump. Studies of polyelectrolytes by conventional electrical discharge temperature-jump instruments can be complicated by electric field effects (Pörschke, 1985; Marcandalli et al., 1984). To avoid this, a Raman laser temperature-jump apparatus (Turner et al., 1972; Turner, 1986) was constructed as shown schematically in Figure 1. A 7-ns, 750-mJ pulse at 1.06 μm from a Quanta-Ray DCR-2A Nd:YAG laser is propagated 10 m and focused with a 1.5-m focal length lens (L1). A 1-m, 4.75 cm diameter Raman cell (Ameen, 1975) filled with 1000 psi of CH_4 is placed 0.5 m from the focusing lens. Stimulated Raman scattering in CH_4 converts about 20% of the energy at 1.06 μm to 1.54 μm. The absorbance of water at 1.06 μm is only 0.067 cm^{-1}, but at 1.54 μm it is 5.32 cm^{-1}. A mirror (M1) placed behind the Raman cell reflects unconverted 1.06-μm light back through the Raman cell and transmits 80% of the 1.54-μm light. Maximum Raman conversion is obtained when M1 is aligned to give a small angle between the incident and reflected beams. Direct reflection must be avoided to prevent damage to laser components. The Raman-shifted pulse is about 5-ns wide. This determines the heating time for the sample. About 120 mJ of 1.54-μm light passes through an area of about 15 mm^2 of the sample cell (C). The cells have open tops and are constructed from Spectrosil quartz. They fit into a Gilford 250 spectrophotometer for easy determination of concentrations. Sample volumes are 15 and 26 μL, respectively, for cells of 0.5- and 1.0-mm path length.

Prior to use, cells are cleaned in a warm solution of KOH in ethanol. A layer of Dow-Corning 200 dimethylpolysiloxane fluid is placed on top of the sample to prevent evaporation. The sample cell is placed in a thermostatically controlled cell holder (A) connected to a circulating bath that maintains the initial sample temperature ±0.1 °C.

Reactions are followed by monitoring the change in absorption with time. The probe source is a 200-W Hg/Xe

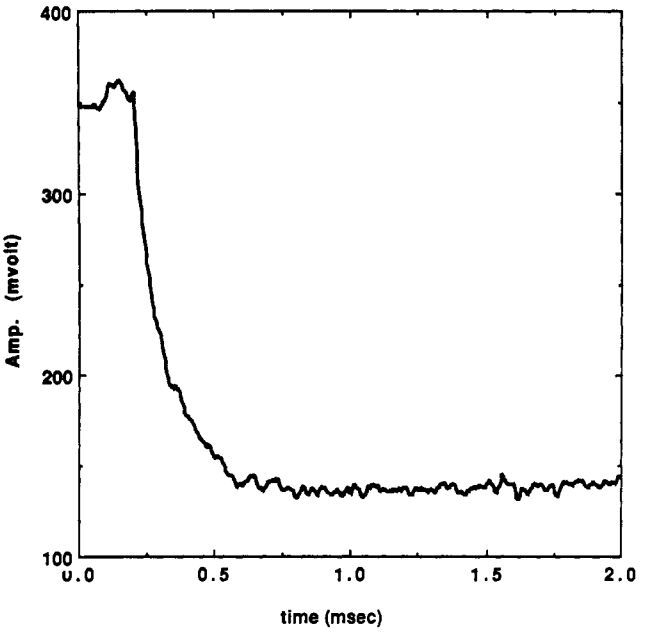

FIGURE 2: Relaxation spectrum of 2.18×10^{-4} M dGCATGC in 1.00 M Na^+ at 45 °C.

Canrad Hanovia arc lamp mounted in a Schoeffel housing. A 10-cm bar magnet is suspended above the lamp to help stabilize arc wander. The lamp is powered by a PRA M304 power supply with a PRA TX-5 optical feedback system that uses the light intensity diverted by beam splitter (B1) to reduce lamp noise. The beam is focused (L2) onto the entrance slit of a Bausch and Lomb high-intensity monochromator set for 260 nm with a band-pass of 9.6 nm. After the monochromator, the beam is collimated by a 15 cm focal length lens (L3) and focused onto the heated region of the sample by a 5 cm focal length lens (L4). A Uniblitz shutter placed between the monochromator and sample is opened 70 ms before the laser pulse and remains open for 100–500 ms. This minimizes exposure of the sample to high-intensity UV light. A beam splitter (B2) is located just before the focusing lens, and the reflection from this is focused by a 9 cm focal length lens (L5) into a reference photomultiplier (D). The light not absorbed by the sample is collected by a 10.5 cm focal length, 7.5 cm diameter lens (L6) and focused with an 11 cm focal length lens (L7) through a Schott UG5 filter onto the sample photomultiplier (E). Both photomultipliers are RCA 1P28's with DIALOG DIA-RMA preamplifiers. The outputs of both photomultipliers are electronically matched and input into a Tektronix 7A22 differential amplifier that subtracts the reference from the sample signal. For signals with relaxation times less than 2 ms, the amplifier is placed in a Tektronix 7912AD digitizer, and the signal is displayed on a Tektronix T922 oscilloscope. Otherwise, the amplifier is placed in a Tektronix 7633 storage oscilloscope and the signal viewed on the screen.

A synchronizing circuit coordinates the opening of the shutter, the triggering of the oscilloscope or digitizer and computer, and the firing of the laser. The data are digitized by either a PDP 11/23 computer or the Tektronix 7912AD digitizer and stored on the computer. With one exception, 512 points were digitzed for relaxations. Data taken over 20 ms consist of only 256 points. Between 4 and 65 curves taken at a repetition rate of 0.2 Hz were averaged per experiment, and each relaxation time represents an average of at least 10 experiments. A typical relaxation spectrum for dGCATGC is shown in Figure 2. Relaxation times were determined with

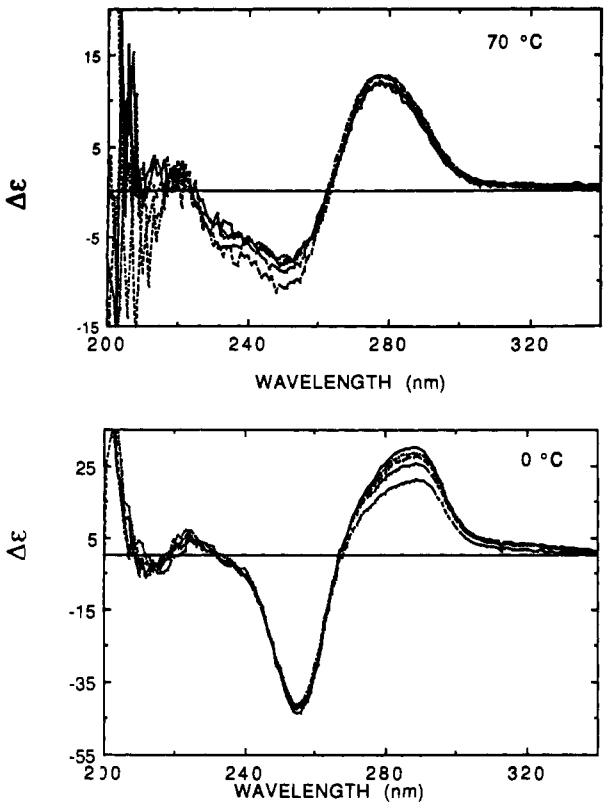

FIGURE 3: CD spectra of 1.1×10^{-4} M dGCATGC at 0 and 70 °C in 1-mm cell. 0 °C spectra [listed in order of $\Delta\epsilon$ (285 nm) from top to bottom]: (–) 0.012 M Na^+; (···) 0.042 M Na^+; (- - -) 0.15 M Na^+; (–·–) 0.012 M Na^+ with 0.01 M Mg^{2+}; (– – –) 1.00 M Na^+.

the multiexponential fitting program DISCRETE developed by S. Provencher (1976).

The temperature change of the instrument was measured by using 6 mM $K_4Fe(CN)_6$. The light intensity, I_0, transmitted by the solution at 275 nm was measured as a function of temperature over a 15 °C range. The relaxation signal amplitude at the midpoint of the temperature range was averaged for 100 experiments and correlated to the change in I_0. The temperature jumps in 0.5- and 1.0-mm path length cells are 1.9 and 1.1 °C, respectively.

Experiments in D_2O provide a convenient control to establish that relaxations observed are due solely to the temperature jump. The absorbance of D_2O at 1.54 μm is only 0.15 cm^{-1} (Thomas et al., 1965). Thus, relaxations due to heating should be absent if D_2O is the solvent. Solutions of 2×10^{-4} M dGCATGC in D_2O buffered at pH 7 with 10 mM sodium cacodylate and 1 mM Na_2EDTA and containing 1 M NaCl or 10 mM $MgCl_2$ or no added salt were studied at 30 °C. No relaxation signals were observed. Thus, the relaxations observed in H_2O solutions are due to the temperature perturbation.

RESULTS

CD Spectra. CD spectra for the duplex and single-strand forms of dGCATGC at 0 and 70 °C, respectively, are shown in Figure 3 for several different salt conditions. Similar spectra are observed for all the salt conditions studied. Evidently, the conformations of both duplex and single strand are relatively insensitive to salt.

NMR Spectra. NMR spectra of nonexchangeable base protons of dGCATGC in 1.0 M NaCl at 23 and 87 °C are shown in Figure 4. The spectrum at 23 °C is similar to that described by Nilges et al. (1987), and their peak assignments have been adopted. Plots of chemical shift vs temperature for

Table I: Melting Temperatures (±2 °C) Derived from dGCATGC ^{1}H NMR Melting Curves

	proton								
	1G8	2C5	2C6	3A2	3A8	4T6	5G8	6C5	6C6
$\Delta\nu$(23 °C)	7.98	5.45	7.50	7.74	8.38	7.13	7.87	5.31	7.40
T_M (°C)	45.7	51.2	54.7	50.1	49.5	51.0	(58.6)	(54.7)	53.5

Table II: Thermodynamic Parameters for Duplex Formation by dGCATGC[a]

		T_M^{-1} vs log C_T				av from fits			
[Na^+] (M)	[Mg^{2+}] (mM)	$-\Delta H°$ (kcal/mol)	$-\Delta S°$ (eu)	$-\Delta G°_{37}$ (kcal/mol)	T_M (°C) (1 × 10^{-4} M)	$-\Delta H°$ (kcal/mol)	$-\Delta S°$ (eu)	$-\Delta G°_{37}$ (kcal/mol)	T_M (°C) (1 × 10^{-4} M)
0.012	0	31.5	88.1	4.21	23.2	42.3	125	3.50	21.8
0.042	0	44.3	128	4.52	29.2	43.2	125	4.58	29.3
0.150	0	47.5	136	5.44	35.5	48.6	139	5.47	35.7
1.00	0	42.4	118	5.85	38.3	46.5	131	5.88	38.4
0.012	2	45.5	131	4.86	31.6	47.2	137	4.81	31.1
0.012	10	45.2	128	5.48	35.7	43.5	122	5.57	36.3
0.150	10	40.8	113	5.71	37.3	48.3	137	5.69	37.1

[a] Errors in $\Delta H°$ and $\Delta S°$ are estimated as ±5%, except for 0.012 M Na^+ in the absence of Mg^{2+}, where errors are estimated as ±10%. Additional significant figures are given to ensure accurate calculation of T_M.

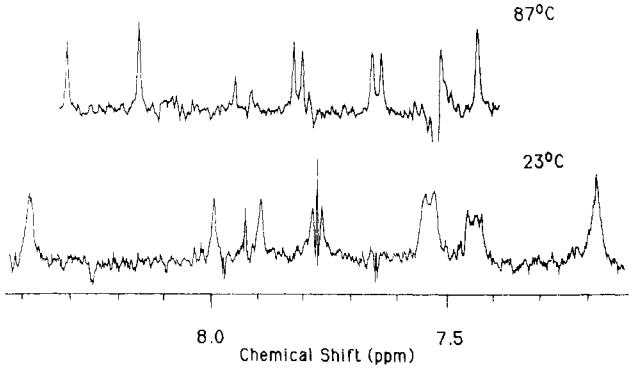

FIGURE 4: NMR spectra of 6.63 × 10^{-4} M dGCATGC in D_2O with 1 M NaCl, 0.01 M sodium cacodylate, and 0.001 M EDTA, pH 7, at 23 (bottom) and 87 °C (top).

the resonances are shown in Figure 5. Melting temperatures determined from these data are listed in Table I. Resonances for the 6C5 and 5G8 protons have sharply sloping base lines, making it difficult to accurately determine T_M's (in parentheses). The T_M's for the other resonances range from 46 to 55 °C with an average of 51 °C. The results are consistent with a two-state melting transition.

Melting Temperature as a Function of Salt. The melting temperature, T_M, as a function of Na^+ concentration is linear for [Na^+] ≤ 0.15 M (see Table II and supplementary material); the slopes, $dT_M/d \log [Na^+]$, are slightly dependent on concentration, 15 and 11 °C, respectively, for 5 × 10^{-6} and 1 × 10^{-4} M dGCATGC. This may reflect the difficulty of determining T_M's below 20 °C for 5 × 10^{-6} M dGCATGC. Melting temperatures were also measured as a function of added Mg^{2+} for 0.012, 0.15, and 1.0 M Na^+. The results are plotted in Figure 6. A linear relationship exists between T_M and log [Mg^{2+}] below 0.03 M Mg^{2+}. The slopes of these lines decrease with increasing Na^+ ion concentration, but are independent of oligomer concentration. In 1.0 M Na^+, the slope is negative, indicating a destabilizing effect of added Mg^{2+}.

The data in Figure 6 also illustrate the effects of Na^+ concentration on T_M when [Mg^{2+}] is held constant. In the presence of less than 10 mM Mg^{2+}, added Na^+ increases T_M, but at a slower rate than in the absence of Mg^{2+}. Above 10 mM Mg^{2+}, added Na^+ either has little effect or decreases T_M.

Thermodynamics. Plots of T_M^{-1} vs log C_T are shown in Figure 7 for 0.012, 0.042, 0.15, and 1.00 M Na^+. Thermodynamic parameters derived from such plots and from averages of individual melting curves are summarized in Table II. The

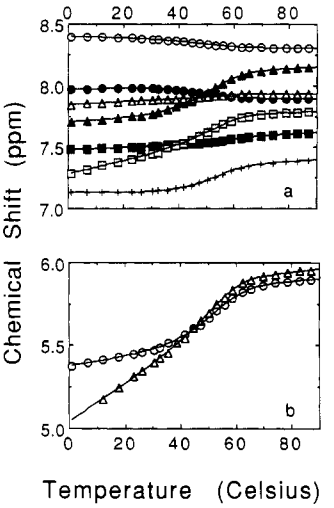

FIGURE 5: NMR chemical shifts vs temperature for 6.63 × 10^{-4} M dGCATGC in D_2O with 1 M NaCl, 0.01 M sodium cacodylate, and 0.001 M EDTA, pH 7. Assigned protons: (a) 1G8 (●), 2C6 (■), 3A2 (▲), 3A8 (○), 4T6 (+), 5G8 (△), 6C6 (□); (b) 2C5 (○), 6C5 (△).

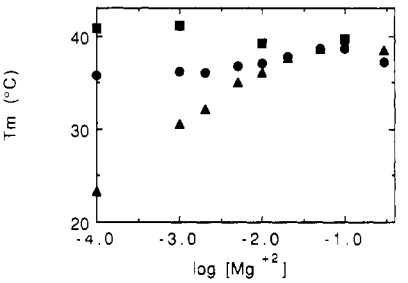

FIGURE 6: Melting temperature, T_M, vs log [Mg^{2+}] for 1 × 10^{-4} M dGCATGC in the presence of 0.012 M (▲), 0.15 M (●), and 1.0 M (■) Na^+.

$\Delta H°$ and $\Delta S°$ of −42.3 kcal/mol and −118 eu, respectively, measured in 1 M Na^+ are close to the values of −42.4 kcal/mol and −121 eu predicted by the nearest-neighbor parameters of Breslauer et al. (1986). Thus, dGCATGC has thermodynamic properties expected for B-form DNA.

Kinetics. Relaxation spectra exhibit a single relaxation time longer than 5 μs corresponding to duplex formation:

$$2\text{dGCATGC} \underset{k_{-1}}{\overset{k_1}{\leftrightarrow}} (\text{dGCATGC})_2 \qquad (1)$$

Table III: Kinetic Parameters for Duplex Formation by dGCATGC[a]

[Na+] (M)	[Mg2+] (mM)	T_M^{-1} vs log C_T temp (°C)	$k_1 \times 10^{-6}$ (s^{-1} M^{-1})	$k_{-1} \times 10^{-2}$ (s^{-1})	av from fits $E_{A,1}$ (kcal/mol)	$E_{A,-1}$ (kcal/mol)	$k_1 \times 10^{-6}$ (s^{-1} M^{-1})	$k_{-1} \times 10^{-2}$ (s^{-1})	$E_{A,1}$ (kcal/mol)	$E_{A,-1}$ (kcal/mol)
0.012	0	20.8	0.33	0.22	15	47	0.31	0.24	10	52
		26.0	0.70	1.2			0.54	1.5		
		31.1	0.98	3.9			0.65	5.9		
		33.9	0.99	6.5			0.61	10		
0.042	0	31.1	1.6	2.1			1.5	2.3		
0.150	0	31.1	7.9	2.6			7.3	2.4		
1.00	0	31.1	9.9	2.2	−5	40	11	1.9	−6	41
		39.4	8.3	14			9.4	12		
		45.0	6.7	39			7.4	35		
0.012	2	32.9	2.6	3.7			2.6	3.8		
0.012	10	31.1	7.3	2.4	−3	43	7.7	2.3	−2	42
		32.9	7.4	3.8			7.8	3.6		
		39.4	7.0	17			7.6	15		
		45.0	6.0	5.2			6.7	4.7		
0.150	10	31.1	9.8	2.6			11	2.3		

[a] Errors in k_1 and k_{-1} are estimated as ±15%.

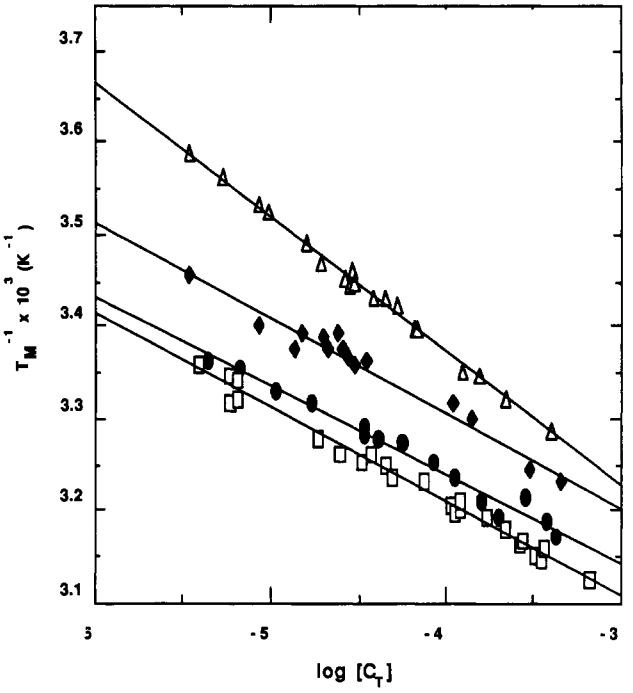

FIGURE 7: Plots of $1/T_M$ vs log C_T for dGCATGC in varying concentrations of Na^+: 0.012 M Na^+ (△); 0.042 M Na^+ (◆); 0.15 M Na^+ (●); 1.00 M Na^+ (□).

The concentration dependence for the relaxation times, τ, for such a reaction is given by

$$\tau^{-2} = 8k_1k_{-1}C_T + k_{-1}^2 \quad (2)$$

Plots of τ^{-2} vs C_T at 31.1 °C for a range of sodium concentrations are shown in Figure 8. Because the intercepts of these plots are small, k_1 and k_{-1} were determined from slopes of the plots and thermodynamic equilibrium constants: $k_1 = (\text{slope} \cdot K_{eq}/8)^{1/2}$ and $k_{-1} = k_1/K_{eq}$. Table III lists rate constants calculated by using equilibrium constants derived from plots of T_M^{-1} vs log C_T and from fits of melting curves.

Arrhenius plots for 0.012 M Na^+, 0.012 M Na^+ with 0.01 M Mg^{2+}, and 1.0 M Na^+ are shown in Figure 9. Activation energies derived from these plots are listed in Table III.

Discussion

The CD and NMR results on dGCATGC indicate it is a suitable system for studying salt effects on duplex formation by oligonucleotides. CD spectra for both single and double strands are relatively insensitive to salt conditions. Thus,

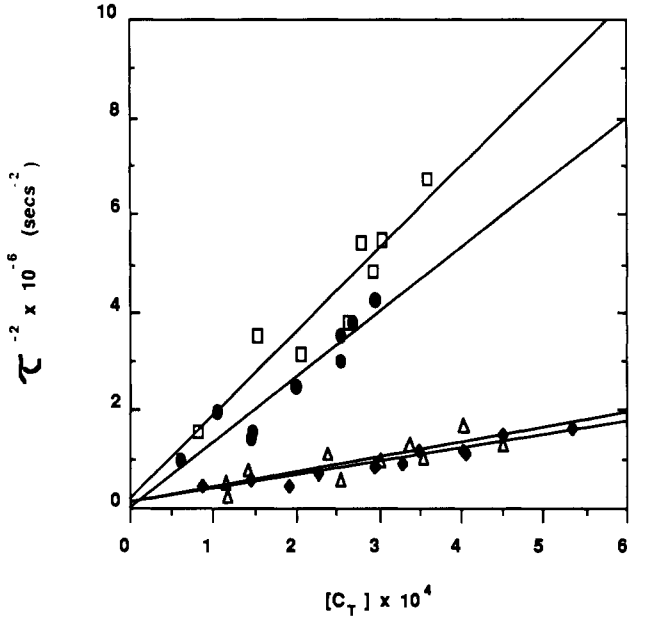

FIGURE 8: Square of the reciprocal relaxation time, τ^{-2}, vs C_T for dGCATGC at 31.1 °C: 0.012 M Na^+ (△); 0.042 M Na^+ (◆); 0.015 M Na^+ (●); 1.00 M Na^+ (□).

results are not complicated by additional salt-induced conformational changes. The NMR results indicate the conformation in 1 M NaCl is similar to that determined previously by Nilges et al. (1987) in 0.5 M KCl. This conformation belongs to the B-form family. The NMR melting results indicate the transition from duplex to single strands in 1 M NaCl is essentially a two-state transition. This also simplifies interpretation of both thermodynamic and kinetic results.

The Dependence of the Melting Temperature of dGCATGC on [Na^+] Is Similar to That Expected for a Polymer. From 0.01 to 0.15 M Na^+, $d(T_M)/d \log [Na^+]$ for 1×10^{-4} M dGCATGC is 11 °C. An even larger $d(T_M)/d \log [Na^+]$ is observed at lower oligomer concentrations, indicating the effect is not due to aggregation. Previous studies on dGCGCGC also showed aggregation only occurs at higher Na^+ and oligomer concentrations (Freier et al., 1983). The strong dependence of T_M on [Na^+] is similar to that observed with polymers of the same base composition. Owen et al. (1969) measured T_M's of naturally occurring DNA's between 0.005 and 0.3 M Na^+. Frank-Kamenetskii (1971) fit these data to an equation that gives $d(T_M)/d \log [Na^+] = 18.30 - 7.04F_{GC}$. Here F_{GC} is the fractional GC content. A similar equation appropriate at 0.14

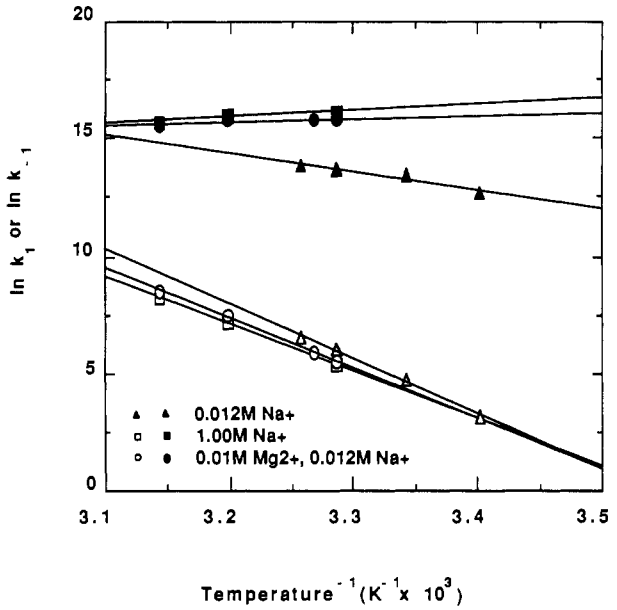

FIGURE 9: Plots of logarithm of the rate constants, ln k, vs reciprocal temperature for dGCATGC. Solid and open symbols are for forward (k_1) and reverse (k_{-1}) rates, respectively. Salt conditions: 0.012 M Na^+ (△, ▲); 1.00 M Na^+ (□, ■); 0.012 M Na^+, 0.01 M Mg^{2+} (○, ●).

M Na^+, $d(T_M)/d \log [Na^+] = 19.96 - 6.65F_{GC}$, was obtained by Blake and Haydock (1979) from studies of subtransitions in the melting of λ DNA. For a polymer with two-thirds GC content, these equations predict $d(T_M)/d \log [Na^+] = 13.6$ and 15.5 °C, respectively. Thus, it appears the melting of polymers and dGCATGC have similar sensitivity to $[Na^+]$ in the absence of Mg^{2+}.

Fewer directly comparable data are available on the salt dependence of polymer T_M's in the presence of Mg^{2+}. In the presence of 0.01 M Na^+, the data of Blagoi et al. (1978) on naturally occurring DNA with about 41% GC content give $d(T_M)/d \log [Mg^{2+}] = 10.2$ and 2.9 °C for $[Mg^{2+}]$ below and above 10^{-4} M, respectively. The data of Krakauer (1974) on poly(A)·poly(U) in 0.0475 M Na^+ give $d(T_M)/d \log [Mg^{2+}] = 12$ °C. For dGCATGC in 0.012 M Na^+, $d(T_M)/d \log [Mg^{2+}] = 6.9$ °C up to 0.1 M Mg^{2+}. Evidently, for dGCATGC the plot of T_M vs log $[Mg^{2+}]$ maintains a constant slope to higher $[Mg^{2+}]$ than that for polymeric DNA. Otherwise, the melting of polymers and that of dGCATGC have similar sensitivity to $[Mg^{2+}]$ in the presence of Na^+.

The sensitivity of T_M to $[Na^+]$ in the presence of Mg^{2+} is somewhat different for dGCATGC and polymeric DNA. For polymeric DNA, increasing $[Na^+]$ decreases T_M after the concentration of Mg^{2+} exceeds half the concentration of DNA phosphate (Record, 1975). For dGCATGC, increasing $[Na^+]$ decreases T_M only after $[Mg^{2+}] \approx 0.1$ M. This is far in excess of the $[Mg^{2+}]$ required to neutralize dGCATGC phosphates.

Although there are some differences, the similarities of the salt dependence for hexamer and polymer melting are surprising. Record and Lohman (1978) derived a theory for electrostatic end effects and calibrated it with the hairpin melting data of Elson et al. (1970). For duplex formation by single strands in the absence of Mg^{2+}, they tentatively predict $\{d(T_M)/d \log [Na^+]\}_N = \{d(T_M)/d \log [Na^+]\}_\infty(1-7.94/N)$, where N is the number of phosphates in the oligomer duplex. The prediction is that $d(T_M)/d \log [Na^+]$ for a hexamer duplex with 10 phosphates should be only one-fifth that observed for the polymer. Instead, it appears to be closer to 1.

The basis for the similarities between oligomer and polymer cannot be determined yet. The salt dependence of polymer melting is described well by counterion condensation and Poisson–Boltzmann theories that predict high local concentrations of counterions around the polymer (Manning, 1978; Record et al., 1978). A key parameter of these theories is the polymer charge density. The NMR results of Nilges et al. (1987) indicate the phosphate spacing in dGCATGC duplex is similar to that in B-form DNA polymers. It would be surprising, however, if electrostatic interactions of a duplex of 10 phosphates were almost identical with those of a polymer. In particular, the condensation effect is expected to be reduced considerably (Record & Lohman, 1978).

One difference between oligomers and polymers that may be important is the phosphate spacing in the single strands. Blake and Haydock (1979) suggest strong stacking in single strands with high GC content may result in a higher charge density than for single strands with high AT content. This would lead to less release of Na^+ on melting and may account for the smaller $d(T_M)/d \log [Na^+]$ observed for GC-rich regions in DNA. If stacking in dGCATGC single strands is less than in the polymer, then the reduced charge density in the single strand would lead to more Na^+ being released on duplex melting of the dGCATGC oligomer. This could partially compensate for reduced counterion condensation around the duplex. Single-strand effects could also rationalize the low value of $d(T_M)/d \log [Na^+]$ predicted by Record and Lohman (1978). Their calibration was based on hairpin formation by oligonucleotides with chain lengths from 18 to 44. Thus, the single strands probably behaved like polymers, whereas dGCATGC single strands may not. Of course, there may be other important differences between oligomers and polymers. Clearly, additional theoretical work is required.

Thermodynamics of Duplex Formation. For six of the seven salt conditions where $\Delta H°$'s and $\Delta S°$'s were determined from shapes of melting curves and from T_M^{-1} vs log C_T plots, the two methods agreed within 15%. This suggests duplex formation under these conditions is a two-state process (Albergo et al., 1981; Petersheim & Turner, 1983; Freier et al., 1986; Turner et al., 1988). The exception is 0.012 M Na^+, where the difference is 25%. This may suggest unusual melting behavior at 0.012 M Na^+. The melting temperatures at 0.012 M Na^+, however, are low, ranging from 6 to 31 °C. This makes it difficult to fit melting curves with certainty. Thus, the different parameters may only reflect the difficulty of the measurement. Fortunately, compensation between $\Delta H°$ and $\Delta S°$ results in less variation in derived $\Delta G°$'s. For 0.012 M Na^+, $\Delta G°$'s at 31 °C determined from curve shapes and T_M^{-1} plots differ by 9%.

The thermodynamic parameters for 0.012, 0.042, and 0.15 M Na^+ can be used to calculate the number of Na^+ ions released upon duplex dissociation (Record et al., 1981):

$$d(\Delta G°)/d \log [Na^+] = -4.6RT(\Psi_h - \Psi_c) \quad (3)$$

Here Ψ_h and Ψ_c are the number of counterions thermodynamically bound per strand to the helix and coil, respectively. From the results in Table II, $\Psi_h - \Psi_c = 0.4$ at 37 °C, giving 0.08 Na^+ ion released/phosphate. This is similar to the average of 0.09 derived for five GC-rich RNA pentanucleotides by using data at 0.01 and 1 M Na^+ (Freier et al., 1984). It is also similar to the 0.096 Na^+ ion released/phosphate measured for dGGAATTCC (Erie et al., 1987). It is somewhat lower than the value of 0.12 Na^+ ion released/phosphate derived by Blake and Haydock (1979) for a λ DNA subtransition with 59% GC content. The results again suggest oligomers behave more like polymers than might be expected.

Thermodynamic Parameters Measured in 1 M NaCl Are Similar to Those Measured in 10^{-3}–10^{-1} M Mg^{2+} in the

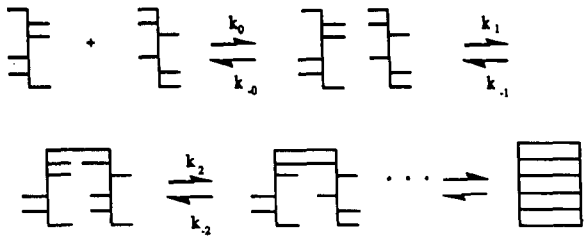

FIGURE 10: Schematic of the Wetmur–Davidson model of duplex formation.

Presence of 0.15–1 M Na^+. Experiments on nucleic acids are carried out under a wide range of salt conditions. Thermodynamic parameters derived from studies of oligo- and polynucleotides are often used to interpret experiments where helix formation is thought to be important. Traditionally, these parameters are measured in 1 M NaCl, and there is little or no evidence concerning applicability under other salt conditions (Tinoco et al., 1973; Breslauer et al., 1986; Freier et al., 1986; Turner et al., 1988). The results in Figure 6 and Table II suggest thermodynamic parameters measured for fully paired duplexes in 1 M NaCl provide reasonable approximations for solutions containing 10^{-3}–10^{-1} M Mg^{2+} in the presence of 0.15–1 M Na^+. For example, the T_M's for 10^{-4} M dGCATGC in 1 M Na^+ and in 0.15 M Na^+ and 10^{-3} M Mg^{2+} are 38 and 36 °C, respectively. Similar differences are observed over the entire indicated range of salt concentrations. Furthermore, except for 0.012 M Na^+, all measured $\Delta H°$'s are within 10% of the average $\Delta H°$ of −45 kcal/mol.

Kinetics of Duplex Formation. Wetmur and Davidson (1968) proposed the mechanism shown in Figure 10 for duplex formation by DNA polymers. The first step in this mechanism is alignment of short stretches of polymer strands to form a nonbonded complex. This is followed by initial base pair formation and then formation of adjacent base pairs until a stable nucleus is present. After formation of the nucleus, subsequent forward rates for addition of adjacent base pairs are faster than reverse rates for breakage of base pairs. Thus, the helix "zips up" from the nucleus. The rate-determining step is formation of the nucleus. A similar mechanism was proposed by Pörschke and Eigen (1971) and by Craig et al. (1971) for duplex formation by oligomers, except the initial alignment step was not considered. The forward rate for this mechanism is given by (Pörschke & Eigen, 1971)

$$k_1 = K_0K_1...K_{n-1}k_{n-1,n} \quad (4)$$

Here K_0, K_1, etc. are equilibrium constants for steps prior to nucleus formation, and $k_{n-1,n}$ is the elementary rate for formation of the nucleus containing n base pairs.

Activation energies for k_1 can provide insight into the number of base pairs required for nucleation (Pörschke & Eigen, 1971; Craig et al., 1971; Pörschke et al., 1973). For the mechanism shown in Figure 10, the activation energy is given by $E_A = \Delta H°_{n-1} + E_{A,n-1\rightarrow n}$. Here $\Delta H°_{n-1}$ is the enthalpy change between single strands and the $n-1$ intermediate; $E_{A,n-1\rightarrow n}$ is the activation energy for the elementary rate between intermediates $n-1$ and n. For dGCATGC in 1 M Na^+ and in 0.012 M Na^+ and 0.01 M Mg^{2+}, the activation energies are about −5 and −3 kcal/mol, respectively. This suggests 3 ± 1 base pairs are required for nucleation. Formation of the intermediate with two base pairs is expected to be associated with a $\Delta H°$ of about −10 kcal/mol (Breslauer et al., 1986). If $E_{A,n-1\rightarrow n}$ is about 5 kcal/mol, then E_A would be about −5 kcal/mol for formation of the third base pair. A value around 5 kcal/mol is reasonable for $E_{A,n-1\rightarrow n}$ since similar activation energies have been measured for stacking in single-stranded polynucleotides (Dewey & Turner, 1979; Freier et al., 1981).

The rate-determining step in 0.012 M Na^+ is less certain. Here, E_A is either 10 or 15 kcal/mol, depending on whether thermodynamic parameters from curve fits or T_M^{-1} plots are used in the data analysis. The positive E_A suggests 2 ± 1 base pairs are rate determining in 0.012 M Na^+. This is based on the assumption that $\Delta H°$ for formation of the first base pair is about 0 kcal/mol. The conclusion is tentative, however. First, the thermodynamic parameters are uncertain. Second, there may be other differences in mechanism between low and high salt. For example, counterion condensation or hairpin formation may be important at low salt, only. A similar change from positive to negative activation energy has been observed for A_7U_7 between 0.25 and 1 M Na^+ (Craig et al. 1971; Breslauer & Bina-Stein, 1977). The results suggest the mechanism for oligomer association changes between low and high salt concentration.

The Dependence of the Association Rate for dGCATGC on [Na^+] Is Very Different from That Observed for Polymers. A plot of log k_1 vs log [Na^+] for duplex formation by dGCATGC is linear between 0.012 and 0.15 M Na^+, with a slope of 0.8 (see supplementary material). A similar plot for A_2GCU_2 between 0.05 and 1.05 M Na^+ gave a slope of 0.6 (Pörschke et al., 1973). Duplex formation by T7 DNA (Studier, 1969) and poly(A)·poly(U) (Ross & Sturtevant, 1960) at somewhat lower [Na^+] gives slopes of about 3.6 (Manning, 1976). Thus, the rate of duplex formation by polymers goes as the 3.6 power of [Na^+], whereas the rates for dGCATGC and A_2GCU_2 go as less than the first power of [Na^+].

Given the similar behavior of $d(T_M)/d \log [Na^+]$ for dGCATGC and polymers, it is initially surprising that the sensitivity of association rate to Na^+ is so different for the two. This dichotomy is expected, however, if the counterion condensation model of Manning (1976, 1978) has relevance for oligomers. Manning has applied polyelectrolyte theory to the mechanism shown in Figure 10 and derives the following equation for the association rate:

$$k_1 = \beta(T;T_M)\gamma_{Na^+}{}^{Q/\xi}[Na^+]^{Q/2\xi} \quad (5)$$

Here β is a proportionality constant, γ_{Na^+} is the activity coefficient for Na^+, Q is the number of phosphate groups lined up in the initial nonbonded complex, and ξ is a dimensionless charge-density parameter equal to $e^2/\epsilon kTb$ (where e is the charge on a proton, ϵ is the bulk solvent dielectric constant, k is Boltzmann's constant, and b is the average distance between the projections of nearest-neighbor charged groups onto the axis of the single-strand chain). From the data of Studier (1969) and Ross and Sturtevant (1960), Manning (1976) derives a value of about 15 nucleotides for Q. That is, 15 nucleotides in each strand are aligned, allowing counterion condensation, before the first base pair is formed. If the mechanism for duplex formation by dGCATGC is the same, then the maximum value possible for Q is 5. Thus, the model predicts that k_1 for dGCATGC will depend on [Na^+] to a power of 3.6(5/15) = 1.2 or less. The measured power of 0.8 is consistent with this prediction.

The dependence of k_1 on salt conditions can also be compared with results expected when ionic strength effects are due solely to Debye–Huckel screening. In this case, the predicted dependence of rate on ionic strength, I, is given by (Weston & Schwarz, 1972; Laidler & Meiser, 1982) $\log k = \log k_0 + 1.02z_Az_B\sqrt{I}$. Here z_A and z_B are the charges on the associating ions. This equation has been shown to agree with experiment for many associations of ions. For dGCATGC between 0.012 and 0.15 M Na^+, a plot of log k_1 vs $\sqrt{I}$ has a slope of 3.3

$M^{-1/2}$. This corresponds to an effective charge of −1.8 per strand. This is less than the formal charge of −5 per strand or the effective charge expected for counterion condensation around the oligomer single strands. Moreover, this model predicts k_1 should depend only on ionic strength. Thus, k_1 should be the same for 0.042 M Na^+ and 0.012 M Na^+ and 0.01 M Mg^{2+}. The k_1's measured at 31 °C for these two conditions differ by more than a factor of 4.

The Rate for Duplex Dissociation Is Relatively Insensitive to Salt Conditions. Whereas the rate for association at 31 °C changes by more than a factor of 10 over the range of salt conditions in this study, the rate for duplex dissociation changes by only about a factor of 3. The fastest k_{-1} is observed with 0.012 M Na^+ and must be treated with caution due to uncertainties in the thermodynamics and mechanism at 0.012 M Na^+. For the other conditions, k_{-1} at 31 °C is almost invariant to salt within experimental error. This is consistent with previous observations on A_2GCU_2 (Pörschke et al., 1973) and with the mechanism in Figure 10 as treated by Manning (1976). In this Manning model, all the counterion condensation occurs in the initial association to form the nonbonded complex. The rate of dissociation, however, depends on the concentration of species containing only the number of base pairs in the nucleus. In Manning's model, breaking of base pairs to form the nucleus in an oligomer will not be associated with loss of counterions. Moreover, the local concentration of counterions around the duplex is expected to be largely independent of the concentration of counterions in the bulk solution. Thus, the relative independence of dissociation rate with salt conditions is consistent with the Manning model.

Conclusion. The salt dependences of the thermodynamic properties of dGCATGC are surprisingly like those of polymers, but the kinetic properties are quite different. Both observations are consistent with expectations from a counterion condensation model for salt effects. The similarity of thermodynamic behavior suggests dGCATGC single strands have a lower charge density than the corresponding polymer and/or end effects are relatively small. The kinetic behavior is consistent with the Wetmur–Davidson–Manning model in which single strands line up to form a nonbonded intermediate that leads to counterion condensation (Wetmur & Davidson, 1968; Manning, 1976). The agreement with expectations from the counterion condensation model is surprising. It seems unlikely that a duplex with 10 phosphates will behave like a polymer. Perhaps other changes on going from polymer to oligomer compensate for reduced counterion condensation. The results also indicate thermodynamic and kinetic parameters measured for fully paired duplexes at 1 M NaCl are a reasonable approximation for a wide range of combinations of Na^+ and Mg^{2+} concentrations.

Supplementary Material Available

Plots of T_M vs log [Na^+] for 5×10^{-6} and 1×10^{-4} M dGCATGC and of log k_1 vs log [Na^+] (2 pages). Ordering information is given on any current masthead page.

Registry No. dGCATGC, 74525-71-6; Na, 7440-23-5; Mg, 7439-95-4.

References

Albergo, D. D., & Turner, D. H. (1981) *Biochemistry 20*, 1413–1418.

Altman, S., Baer, M., Guerrier-Takada, C., & Vioque, A. (1986) *Trends Biochem. Sci. 11*, 515–518.

Ameen, S. (1975) *Rev. Sci. Instrum. 46*, 1209–1215.

Barone, A. D., Tang, J. Y., & Caruthers, M. H. (1984) *Nucleic Acids Res. 12*, 4051–4061.

Beaucage, S. L., & Caruthers, M. H. (1981) *Tetrahedron Lett. 22*, 1859–1862.

Blagoi, Y. P., Sorokin, V. A., Vaceyev, V. A., Khomenko, S. A., & Gladchenko, G. O. (1978) *Biopolymers 17*, 1103–1118.

Blake, R. D., & Haydock, P. V. (1979) *Biopolymers 18*, 3089–3109.

Borer, P. N., Dengler, B., Tinoco, I., Jr., & Uhlenbeck, O. C. (1974) *J. Mol. Biol. 86*, 843–853.

Borer, P. N. (1975) in *Handbook of Biochemistry and Molecular Biology: Nucleic Acids* (Fasman, G. D., Ed.) 3rd ed., Vol. 1, p 589, CRC, Cleveland, OH.

Breslauer, K. J., & Bina-Stein, M. (1977) *Biophys. Chem. 7*, 211–216.

Breslauer, K. J., Sturtevant, J. M., & Tinoco, I., Jr. (1975) *J. Mol. Biol. 99*, 549–565.

Breslauer, K. J., Frank, R., Blöcker, H., & Marky, L. A. (1986) *Proc. Natl. Acad. Sci. U.S.A. 83*, 3746–3750.

Burke, J. M., Irvine, K. D., Kaneko, K. J., Kerker, B. J., Oettgen, A. B., Tierney, W. M., Williamson, C. L., Zaug, A. J., & Cech, T. R. (1986) *Cell 45*, 167–176.

Cech, T. R. (1987) *Science 236*, 1532–1539.

Craig, M. E., Crothers, D. M., & Doty, P. (1971) *J. Mol. Biol. 62*, 383–401.

Dewey, T. G., & Turner, D. H. (1979) *Biochemistry 18*, 5757–5762.

Elson, E. L., Scheffler, I. E., & Baldwin, R. C. (1970) *J. Mol. Biol. 54*, 401–415.

Erie, D., Sinha, N., Olson, W., Jones, R., & Breslauer, K. (1987) *Biochemistry 26*, 7150–7159.

Frank-Kamenetskii, M. D. (1971) *Biopolymers 10*, 2623–2624.

Freier, S. M., Hill, K. O., Dewey, T. G., Marky, L. A., Breslauer, K. J., & Turner, D. H. (1981) *Biochemistry 20*, 1419–1426.

Freier, S. M., Albergo, D. D., & Turner, D. H. (1983) *Biopolymers 22*, 1107–1131.

Freier, S. M., Petersheim, M., Hickey, D. R., & Turner, D. H. (1984) *J. Biomol. Struct. Dynam. 1*, 1229–1242.

Freier, S. M., Kierzek, R., Jaeger, J. A., Sugimoto, N., Caruthers, M. H., Neilson, T., & Turner, D. H. (1986) *Proc. Natl. Acad. Sci. U.S.A. 83*, 9373–9377.

Hickey, D. R., & Turner, D. H. (1985) *Biochemistry 24*, 2086–2094.

Ikuta, S., Chattopadhyaya, R., & Dickerson, R. E. (1984) *Anal. Chem. 56*, 2253–2256.

Krakauer, H. (1971) *Biopolymers 10*, 2459–2490.

Krakauer, H. (1974) *Biochemistry 13*, 2579–2589.

Laidler, K. J., & Meiser, J. H. (1982) *Physical Chemistry*, pp 388–390, Benjamin/Cummings, Menlo Park, CA.

Manning, G. S. (1976) *Biopolymers 15*, 1333–1343.

Manning, G. S. (1978) *Q. Rev. Biophys. 11*, 179–246.

Marcandalli, B., Winzek, C., & Holzwarth, J. F. (1984) *Ber. Bunsen-Ges. Phys. Chem. 88*, 368–374.

Matteucci, M. D., & Caruthers, M. H. (1981) *J. Am. Chem. Soc. 103*, 3185–3191.

Nilges, M., Clore, G. M., Gronenborn, A. M., Brunger, A. T., Karplus, M., & Nilsson, L. (1987) *Biochemistry 26*, 3718–3733.

Owen, R. J., Hill, L. R., & Lapage, S. P. (1969) *Biopolymers 7*, 503–516.

Petersheim, M., & Turner, D. H. (1983) *Biochemistry 22*, 256–263.

Pörschke, D. (1985) *Annu. Rev. Phys. Chem. 36*, 159–178.

Pörschke, D., & Eigen, M. (1971) *J. Mol. Biol. 62*, 361–381.
Pörschke, D., Uhlenbeck, O. C., & Martin, F. H. (1973) *Biopolymers 12*, 1313–1335.
Provencher, S. W. (1976) *J. Chem. Phys. 64*, 2772–2777.
Record, M. T., Jr. (1975) *Biopolymers 14*, 2137–2158.
Record, M. T., Jr., & Lohman, T. M. (1978) *Biopolymers 17*, 159–166.
Record, M. T., Jr., Anderson, C. F., & Lohman, T. M. (1978) *Q. Rev. Biophys. 11*, 103–178.
Record, M. T., Jr., Mazur, S. J., Melancon, P., Roe, J. H., Shaner, S. L., & Unger, L. (1981) *Annu. Rev. Biochem. 50*, 997–1024.
Reich, C., Olsen, G. J., Pace, B., & Pace, N. R. (1988) *Science 239*, 178–181.
Richards, E. G. (1975) in *Handbook of Biochemistry and Molecular Biology*: *Nucleic Acids* (Fasman, G. D., Ed.) 3rd ed., Vol. 1, p 597, CRC, Cleveland, OH.
Ross, P. D., & Sturtevant, J. M. (1962) *J. Am. Chem. Soc. 84*, 4503–4507.
Studier, F. W. (1969) *J. Mol. Biol. 41*, 199–209.
Sugimoto, N., Kierzek, R., & Turner, D. H. (1988) *Biochemistry 27*, 6384–6392.
Thomas, M. R., Scheraga, H. A., & Schreier, E. E. (1965) *J. Phys. Chem. 69*, 3722–3726.
Tinoco, I., Jr., Borer, P. N., Dengler, B., Levine, M. D., Uhlenbeck, O. C., Crothers, D. M., & Gralla, J. (1973) *Nature, New Biol. 246*, 40–41.
Turner, D. H. (1986) in *Investigations of Rates and Mechanisms of Reactions* (Bernasconi, C. F., Ed.) Vol. 6, Part 2, Wiley, New York.
Turner, D. H., Flynn, G. W., Sutin, N., & Beitz, J. V. (1972) *J. Am. Chem. Soc. 94*, 1554–1559.
Turner, D. H., Sugimoto, N., Kierzek, R., & Dreiker, S. D. (1987) *J. Am. Chem. Soc. 109*, 3783–3785.
Turner, D. H., Freier, S. M., & Sugimoto, N. (1988) *Annu. Rev. Biophys. Biophys. Chem. 17*, 167–192.
Weston, R. E., Jr., & Schwarz, H. A. (1972) *Chemical Kinetics*, pp 165–171, Prentice-Hall, Englewood Cliffs, NJ.
Wetmur, J. G., & Davidson, N. (1968) *J. Mol. Biol. 31*, 349–370.

Secretagogue-Induced Diacylglycerol Accumulation in Isolated Pancreatic Islets. Mass Spectrometric Characterization of the Fatty Acyl Content Indicates Multiple Mechanisms of Generation†

Bryan A. Wolf, Richard A. Easom, Jonathan H. Hughes, Michael L. McDaniel, and John Turk*
Division of Laboratory Medicine, Departments of Medicine and Pathology, Washington University School of Medicine, St. Louis, Missouri 63110

Received December 9, 1988; Revised Manuscript Received February 7, 1989

ABSTRACT: Diacylglycerol accumulation has been examined in secretagogue-stimulated pancreatic islets with a newly developed negative ion chemical ionization mass spectrometric method. The muscarinic agonist carbachol induces islet accumulation of diacylglycerol rich in arachidonate and stearate, and a parallel accumulation of ^{3}H-labeled diacylglycerol occurs in carbachol-stimulated islets that had been prelabeled with [^{3}H]glycerol. Islets so labeled do not accumulate ^{3}H-labeled diacylglycerol in response to D-glucose, but D-glucose does induce islet accumulation of diacylglycerol by mass. This material is rich in palmitate and oleate and contains much smaller amounts of arachidonate. Neither secretagogue influences triacylglycerol labeling, and neither induces release of [^{3}H]choline or [^{3}H]phosphocholine from islets prelabeled with [^{3}H]choline. These observations indicate that the diacylglycerol that accumulates in islets in response to carbachol arises from hydrolysis of glycerolipids, probably including phosphoinositides. The bulk of the diacylglycerol which accumulates in response to glucose does not arise from glycerolipid hydrolysis and must therefore reflect de novo synthesis. The endogenous diacylglycerol which accumulates in secretagogue-stimulated islets may participate in insulin secretion because exogenous diacylglycerol induces insulin secretion from islets, and an inhibitor of diacylglycerol metabolism to phosphatidic acid augments glucose-induced insulin secretion.

The biochemical events which regulate insulin secretion from the β cells of pancreatic islets are at present incompletely understood. Two general classes of insulin secretagogues are recognized (Wollheim & Sharp, 1981; Prentki & Matschinsky, 1987). One class induces secretion by interaction with β-cell plasma membrane receptors. Muscarinic agonists including acetylcholine and carbachol are examples of insulin secretagogues from this class. A second class of insulin secretagogues is metabolized by glycolytic and/or tricarboxylic acid pathways in islets and may induce secretion by virtue of their utilization as fuels (Malaisse et al., 1979; Hedeskov, 1980; Ashcroft, 1980; Meglasson & Matschinsky, 1986). D-Glucose is an example of such a fuel secretagogue and is the predominant physiologic regulator of insulin secretion. Elucidation of the biochemical mechanisms underlying glucose-induced insulin secretion remains an important objective because there is a relatively selective impairment in glucose-induced insulin secretion in the disease type II diabetes mellitus despite nearly normal insulin secretory responses to some other secretagogues (Pfeiffer et al., 1981).

† These studies were supported by grants from the U.S. Public Health Service (Grants RO1-DK-34388, KO4-DK-01553, RO1-DK-06181, S10-RR-04693, and RR-00954), from the Council for Tobacco Research (Grant 2364), and from the Juvenile Diabetes Foundation International (Grant 188471).

* To whom correspondence should be addressed at Box 8118, Washington University School of Medicine, 660 South Euclid Ave., St. Louis, MO 63110.

0006-2960/89/0428-4291$01.50/0